PERFORMANCE OF MULTIPLE EMISSION PEAK LIGHT EMITTING DIODE LIGHT CURING UNIT: DEGREE OF CONVERSION AND MICROHARDNESS OF RESIN-BASED PIT AND FISSURE SEALANT.

BY:
IBRAHIM BA ARMAH

Submitted to the Graduate Faculty of the School of
Dentistry in partial fulfillment of the requirements
for the degree of Master of Science in Dentistry,
Indiana University School of Dentistry, July 2022.

Thesis accepted by the faculty of the Department of Operative Dentistry, Indiana University, in partial fulfillment of the requirements for the degree of Master of Science in Dentistry.

Armando E. Soto
Chair of the Research Committee

Jeffrey A. Platt
Research Committee Member

Laila A. Al Dehailan
Research Committee Member

July 13, 2022
Date

DEDICATION

I would like to thank and show gratitude to Allah for his many blessings, graces, and virtues. "All the praises and thanks be to Allah, who has guided us to do this, and never could we have found guidance, were it not that Allah had guided us". "All praise is due to Allah with whose favors all good can be accomplished". "My lord, grant me the power and ability that I may be grateful for your favor which you have bestowed upon me".

All my thanks, gratitude, and prayers go to my beloved parents, who taught me, supported me, and kept me going; they made possible what is impossible and difficult, so that I can accomplish my dreams and reach my goals; and I know that their happiness when I succeed exceeds my happiness. May Allah bless them and grant them happiness.

My thanks go to my dearest sisters and brothers, for their love, support and encouragement. I hope we can meet soon beneath one roof as we used to do every weekend; I really miss that.

All my thanks go to my supportive friends, and to those people who care about me and encouraged me throughout my journey.

ACKNOWLEDGMENTS

I would like to convey my deepest gratitude to Imam Abdulrahman bin Faisal University for giving me the opportunity to continue my graduate studies.

My appreciation and gratitude go to my research committee starting with my mentor, Dr. Armando E. Soto. I thank him for his valuable guidance, knowledge, and efforts. My sincerest gratitude goes to Dr. Jeffrey Platt and Dr. Laila Al Dehailan for their helpful suggestions, knowledge and support that guided me to finish my research.

Finally, I would like to thank also the statisticians, George Eckert for his support. I also would like to express appreciation to all my professors in the school for teaching me what was helpful in obtaining my degree.

TABLE OF CONTENTS

LIST OF TABLES AND ILLUSTRATIONS

INTRODUCTION

On caries susceptible tooth surfaces, dental pit and fissure sealants are applied to form a protective layer against food, dental plaque and cariogenic bacteria. Resin based pit and fissure sealants that are widely used have low viscosity resin and are polymerized by visible light exposure. Pit and fissure sealants bond micromechanically to the tooth surface acting as a physical barrier that blocks nutrition sources preventing biofilm growth (1-3).

Nowadays pit and fissure sealants present as two types, resin-based sealants and glass ionomer-cement-based sealants. Resin-based sealants available today are categorized mainly depending on their components (4-10)

The light-cured resin-based sealants are cured by the light activation of the resin materials mostly using camphorquinone (CQ) -aliphatic amine initiators systems to start the polymerization process. CQ photoinitiators commonly exhibit a limited absorbance range of 465 to 470 nm in the visible range of blue wavelengths, whereas alternative photoinitiators sometimes used have an absorption spectrum in the near UV region between 380 and 420 nm, with a limited absorbance range of 395-410 nm in the visible blue range (11). A new generation of Light Emitting Diode Light Curing Units (LED LCUs) with multiple emission peaks (multiwave) have been developed as having two narrow peaks within a range between 395 nm and 510 nm that are designed to meet the absorption spectrum of CQ and other photoinitiators. An outstanding performance was observed with the latest generations of these multiwave LED LCUs when compared to older curing light units that provide monowave LED output (12, 13). The ability of the curing light tip to transmit light to the polymerization process still plays a critical role. The distance between the curing light tip and resin-based material has a significant role on the polymerization process. As the distance between the curing light tip and the surface increases, a significant decrease in irradiance occurs. The radiant exposure of resin-based materials (J/cm^2) refers to the amount of energy that is transmitted to their surface. The radiant exposure is the product of irradiation time and light irradiance expressed in terms of electromagnetic radiation power per square meter (J/cm^2) (14).

Multiple studies have shown that radiant exposure has a significant impact on material properties. The degree of conversion (DC) of a resin material is presumed as linearly proportionate to the light emission time. Hence, investigation of the quickest light emission time that will yield the highest DC without impairing the resin's physical properties is rational (15, 16). As the term implies, the degree of conversion (DC) is the proportion of the carbon-carbon double bonds (C=C) present in monomers that are subsequently converted into carbon-carbon single bonds (C-C) to form the structure of the polymer as a result of polymerization of the resin. Attenuated total

reflection-Fourier transform infrared spectroscopy (ATR-FTIR) is well established as a reliable method for determining DC for resin-based materials, as it identifies the C=C stretching vibrations prior to and following polymerization of resin materials. Effective hardness among a wide range of mechanical properties requires a high percentage of DC (17, 18). An indirect method to assess the level of degree of conversion is through microhardness by calculating the ratio of the bottom to top surface values. There should be no difference in the values of the hardness of the top surface and the bottom surface of more than 20 percent between these ratios (19). Despite this, the microhardness and DC relationship is not fully predictable as the microhardness can be affected by other factors than DC. There is no quantitative information in the microhardness test results regarding the actual change in the reactive groups (20).

Even though some may consider pit and fissure sealant placement as easy, it is still a very technique sensitive procedure to reduce the need of repair or replacement of the sealants. As an example, since its foundation in 2003, the Indiana University School of Dentistry (IUSD) Seal Indiana program completed over 35,000 sealants, but numerous of the sealants placed are replacements. During 2007-2009, 834 children were assessed, and 940 sealants were placed with 518 (61%) of these sealants being either repairs or replacements. Alongside adequate wave-lengths necessary to activate the photoinitiators in the sealant material, proper intensity is also needed for an effective polymerization process since filler content, translucency, and the material's thickness affect light transmission. Additionally, the distance between the light curing tip and the resin surface as well as the exposure period are also crucial for degree of conversion and can be modified by the practitioner to considerable magnitude. Sufficient curing is crucial for the successful and long-term performance of pit and fissure sealants (21, 22).

Unsatisfactory polymerization of the resin matrix might yield the resin pit and fissure sealant material more susceptible to the plasticizing effect of exogenous substances which include a variation of chemicals such as acids, bases, salts, alcohols or oxygen that may enter the oral environment thru eating or drinking and could result in a degrading effect on the resin and weaken its clinical effectiveness (23-27). Results obtained from our study would contribute to our understanding of the degree of conversion in resin-based pit and fissure sealants curable with multi wave LED LCUs, which can aid dental professionals in determining if 1000 mW/cm^2, 1400 mW/cm^2 or 3200 mW/cm^2 irradiance power on a specific LED LCU is appropriate for effective and anticipated clinical outcomes for the pit and fissure sealant used in this study. A previous study reported DC values ranging from 51-55% in resin-based pit and fissure sealants (27). Another study reported DC values of 77% to 86% while a third study reported DC values of pit and fissure sealants to be approximately 45% (28, 29). Previous clinical studies focused on comparing

different types of fissure sealants (30, 31) and evaluated different adhesive systems used with fissure sealants (32). Another review suggested that further research is needed to determine the properties such as retention of fissure sealants (7). A review of the literature demonstrated no clinical studies testing different irradiance levels on the fissure sealant properties.

Previous studies tested degree of conversion and microhardness of pit and fissure sealants using one type of light curing unit with curing time and distance as variables, tested different types of pit and fissure sealants, combined the comparisons of different sealants and different curing time and distances, or compared the effect different light curing units (quartz-tungsten-halogen compared to Light Emitting Diode) (13, 27, 33). In this study, there was on test a single type of pit and fissure sealant with one light curing unit that had three different irradiances at standardized distances and for two different curing times for each irradiance, as previous studies resulted in conflicting results on the matter of increasing the irradiance and shortening the time of cure (34, 35).

Our aim by the end of this project was to determine how using high irradiance and shortening the time of cure will affect the mechanical properties of the fissure sealants and the significance of different irradiance levels on these properties. This would provide guidance for clinicians performing fissure sealant procedures to understand what level of irradiances and curing times are appropriate for effective polymerization for the fissure sealant used in this study.

REVIEW OF LITERATURE

From a primary prevention point of view, the pits and fissures found on the occlusal surfaces of permanent molars and the palatal surfaces of some maxillary incisors tend to accumulate food remnants and promote the adherence of bacterial biofilm which increases the risk of the development of carious lesions. Sealing these occlusal surfaces effectively with pit and fissure sealants can prevent caries. In addition to their use for primary prevention, research shows pit and fissure sealants can decrease the progression of non-cavitated carious lesions. Knowing sealants can inhibit the progression of carious lesions is critical to the dentist when determining the proper intervention for non-cavitated carious lesions (36).

Regarding the materials used for pit and fissure sealants, they can be classified into four predominant types: resin-based, glass ionomer cement, polyacid-modified resin, and resin-modified glass ionomer. Commonly used are the resin-based sealants. Resin-based sealant monomers are mainly urethane dimethacrylate (UDMA), or bisphenol A-glycidyl methacrylate (bis-GMA) which polymerize by a chemical activator or by light activation of a specific wavelength and power. Resin-based pit and fissure sealants come in different varieties as unfilled, filled, clear or opaque materials (25, 37). Sealants have developed over the past few decades, beginning with the earliest generation of UV-activated sealants, continuing to subsequent generations of chemically-polymerized and light-polymerized sealants, and ending with the generation of fluoride-containing sealants. The first generation of sealants are not on the market anymore (6, 7, 38). The most commonly used sealants are light cured resin-based materials, which are light polymerized resin materials using CQ-aliphatic amine initiators. Alternative photoinitiators such as 2,4,6-trimethylbenzoyldiphenylphosphine oxide (TPO) are used alongside CQ or sometimes as substitute photoinitiators. (39).

Aromatic or aliphatic dimethacrylate monomers are usually the components of the resin matrix that composes resin-based pit and fissure sealant materials. To transform the monomers into a complex polymer structure an adequate light activation is required (35). The polymerization process of resin-based material activated by the absorption of light in a certain range of wavelength results in reaction with the reducer agent (aliphatic amine) to create free radicals. As the term implies, the degree of conversion (DC) is the proportion of the carbon double bonds (C=C) present in monomers that are subsequently converted into carbon single bonds (C-C) to form the chain of the polymer as a result of polymerization of the resin. An

important factor contributing to the physical and mechanical properties of resins is the percentage of monomers converted to polymers during the polymerization process (40, 41).

The degree of conversion is calculated by comparing the amount of remaining double bonds in the polymer structure to the initial amount. This ratio is expressed in % and termed the degree of conversion (DC) (42). The percentage of DC varies from 35 to 77% for a wide variety of resin materials (43). Gelation occurs as a result of the rapid growth of the system viscosity following photopolymerization, as the conversion rate and cross-link density increase and a viscous liquid to an elastic gel is formed (44).

However, the diffusion of small monomer molecules is still possible in the gelation stage while the diffusion of radicals located on large molecules are mostly restricted. Subsequently, bimolecular termination declines drastically although new growth centers continue to be generated during this process (42).

As a result of the increased concentration of free radicals, an auto-acceleration occurs leading to an increased acceleration of polymerization (Rp, the ratio at which the bond between two molecules is transformed per second, represents the speed of this process) (45). A significant decline in Rp occurs as the viscosity increases, which limits even the diffusion of monomer molecules. Consequently, the rubbery state will change to a glassy state, also known as vitrification (46). Vitrification prevents any additional reactions and causes DC to fail to reach 100%, even when irradiation is carried out according to ideal conditions (47).

In the 1970s, the first dental curing light was developed by Dentsply/Caulk, was called the Nuva Light and used ultraviolet light. Due to adverse biological effects and poor tooth structure penetration, the ultraviolet light was discontinued and replaced with systems activated by visible blue light in the 1980s (25). The earliest replacements were quartz–tungsten–halogen (QTH) lights (48). In 1998 the plasma arc curing light was introduced (49). The light-emitting-diode (LED) curing light was the latest innovated technology in this area. This LED technology became a popular alternative to the use of conventional QTH lights. The LED curing lights produce a narrow spectral range that require less operating power and generate less internal heat. LEDs also have long lasting diodes and they can be cordless containing rechargeable batteries

(50). Compared with QTH, the early generations of LEDs did not always perform as well when the photoinitiator of the material was activated by light at wavelengths shorter than CQ (51-53). Currently many companies are advertising newer generations of LED lights that are capable of higher levels of output as well as a broader range of peak wavelengths (54). The absorbance peak of CQ is from 465 to 470 nm, to match this limited absorption peak the manufacturers made LCUs with a single emission peak within the range of 420 to 490 nm at blue wavelengths. The substitute photoinitiators have absorption spectra that extend from three-hundred-nm violet light to 420-nm violet visible light having a distinct absorption peak (395-410 nm) (11). To address the drawback of the emission absorbance gap of materials that contain substitute photoinitiators, manufacturers introduced multi-wave LED LCUs which have two peaks within the range of 395 to 510 nm that correspond to the absorption spectrum of CQ and the substitute photoinitiators (12, 13)

The efficiency of photopolymerization can be assessed by testing various properties. DC is one of the most important properties of interest since it has a direct correlation with mechanical properties (55, 56), volumetric shrinkage (57), wear resistance (58), and monomer elution (59). Infrared Fourier transform spectroscopy or Raman spectroscopy are the most common spectroscopic techniques used to measure DC. By increasing the DC of the resin system, the mechanical properties will be improved, thereby enhancing the restoration's longevity (60).

The degree of conversion has been correlated to the microhardness of a resin-based material. The Knoop hardness value (KHN) reflects the estimated DC of a resin under various circumstances. Microhardness bottom/top ratios (KHN B/T ratios) can be used to test the influence of the light source on the DC (61). Microhardness measurements (either Vickers or Knoop microhardness) have also been indirectly used to evaluate the DC as a good linear correlation has been observed between DC and microhardness values (62, 63). Several oppose using this relationship as a general rule since other factors than DC affect the microhardness (64). Either way, microhardness measurements do not specify specific data on the changes that are occurring in reactive groups (42). Furthermore, other characteristics may also be considered as indirect evaluation methods, such as degree of crosslinking (65), mechanical properties (66, 67), shrinkage and shrinkage stress (56), depth of cure (68), trapped free radicals (69), and biocompatibility (17).

Factors intrinsic or extrinsic to the photopolymerization process can affect its DC. Photoinitiator systems are considered as intrinsic factors and the most commonly used photoinitiator system in the resin-based materials is a combination of CQ and an electron donor, or co-initiator, each of which is an aliphatic amine (70, 71). It has been found that increasing the photoinitiator concentration increases DC and hardness (72, 73). The results indicated that the DC and hardness decreased as the CQ or amine levels were increased beyond optimum values. This may be because there is a greater concentration of light in the upper portions, which results in decreased light diffusion to the lowest. The use of tertiary photoinitiator systems, such as iodonium salts of amines, will further increase polymerization rate, DC, cross-linking, mechanical properties, and color durability (74-76).

There are intrinsic factors that can affect photopolymerization efficiency, such as viscosity, monomers, and fillers. As the evidence suggests, the viscosity of the resin is a crucial factor in the kinetics of dimethacrylate polymerization, since it impacts each monomer's mobility and reactivity (46). The viscosity of the resin-based material, the filler, the molecular structure of the monomer (such as polymethacrylates or di-methacrylates), as well as their proportions, can affect polymerization efficiency (42). The maximum polymerization is less than 5% conversion in pure bis-GMA, which is caused by its very high viscosity, and the final density is 30% or more. On the other hand, the maximum polymerization for triethyleneglycol dimethacrylate TEGDMA, due to its low viscosity, is found to be around 22% conversion, and has a DC of more than 60%, whereas the different monomer combinations in the polymer exhibit a range of values that are in between these two degrees (77). The polymerization efficiency can be significantly affected by the content of the fillers (42). A study found that for a given resin, formulation and differences in filler sizes and geometries within a filler volume (56.7%) contributed significantly to DC, ranging from 48 to 61% (78).

Finally, resin composites' optical properties are directly related to their photopolymerization processes (42). In a resin-based material, light transmission can be limited by two factors. The first is the reflection of light by the resin surface (79, 80).The second is absorption of light, caused by pigments, which is the reason why dark and opaque shades of resin exhibit a lower depth of cure, or by photo-initiators (65, 78, 81, 82).

Photopolymerization efficiency is also affected by extrinsic factors as well as the intrinsic factors that were reviewed earlier. There are some extrinsic factors such as light curing units and emission spectrum that could alter the of photopolymerization efficiency. As discussed previously, there has been a wide variety of light curing units with different efficiencies employed in the process of photopolymerization (83-87). The first-generation LEDs were made available in the marketplace by the end of 2000. LED technology creates light that releases only in the blue part of the spectral radiation between 440-480 nm without any filtering (25). LED technology has several advantages compared to other LCUs such as low wattage requirement, battery operation, and no noise generated by fans. In the newest generation of LED curing lights, LED chips are combined to boost intensity and wavelength range (25) Compared with older curing light units, the newest generations of LED curing lights display an outstanding performance (88). Yet, the amount of light emitted by the curing tip still contributes to polymerization efficiency (44). As the distance between the curing light tip and the surface increases, the irradiance decreases significantly. With the aim of increasing the light transmission, well-collimated straight light guides have been used to decrease light loss by concentrating rays on a smaller area (89). Additionally, it's possible that there is a heterogeneity in the cure over the surface due to either an array of different diodes or an uneven distribution of the light in the tip (89, 90). As a result of the use of mixing tubes and diffusing screens, the homogeneity of light intensity is improved (90). LED lights polymerize CQ-based materials more efficiently than broad spectrum halogen lights because the blue light spectrum is focused on CQ’s peak absorption, therefore the cure time is reduced. While light sources with broad spectrums may be required by different photoinitiator systems (18, 81).

Photopolymerization efficiency might be influenced by other external factors like radiant exposure. Radiant exposure (J/cm^2) is defined as the total amount of energy brought to the resin materials' surface. Radiant exposure is determined by time and light irradiance (mW/cm^2) that is expressed as the power of electromagnetic radiation per unit area. The radiant exposure is considered the main affecting factor of the material properties (91, 92), Localized variables in irradiance and wavelength distribution may cause a significant effect on the relevance of measurements made to describe the properties of a light cured resin material (81, 90, 93-97). Certain regions of the light tip could transmit a high amount of light, while others may transmit

very little light with a completely different spectrum. The resin-based material will receive insufficient irradiance or light emission from the LCU if there is heterogeneity in the light beam. This may result in misleading results. It has been demonstrated that the resin-based light curing material would scatter light to some extent, but somehow modulating the effects of beam heterogeneity and beam profile can be observed in the distribution of microhardness in the resin light cured material (81, 90, 93, 98).

The modes of irradiation have been considered as extrinsic factors which could influence the photopolymerization process. Several “soft-start” modes (ramp, step or pulse-delay modes) have been suggested. The aim of soft start curing modes was to reduce the polymerization shrinkage stresses by delaying the onset of polymer gelation to allow the polymer to polymerize at a low initial rate. Some studies have shown that soft-start modes reduce shrinkage stress while preserving mechanical properties and DC (99-102). However, it is possible that the inconclusive results are a result of disparities in the compositions between different resin materials that were evaluated in these studies, thus influencing their efficacy and properties during the soft-start curing mode.

In addition, temperature plays an important role in polymerization. The temperature transition from an average room temperature of 22 °C to the temperature of the mouth, with an average of 35 °C, resulted in an increase in hardness, polymerization rate, and DC (6–10%) (103). Thus, as temperature increases, more of the reaction occurs before vitrification. Therefore, temperature constancy should be considered when testing resin-based materials (104).

From a clinical point of view the angulation and position of the LCU could have a significant impact on the amount of irradiance and wavelength emitted to the various spots of the resins (105). Thus, the angulation and position of the LCU could be regarded as an extrinsic factor contributing to the effectiveness of the polymerization process. There is an inverse relationship between irradiance and the distance between the LCU tip and the restoration, resulting in decreased DC (106, 107). For this reason, manufacturers recommend positioning the LCU’s tip as close as possible to the restoration. Furthermore, a constant and perpendicular direction to the restoration is believed to be an effective factor to ensure polymerization depth (108).

GENERAL AIM

The aim of this study was to assess the effect of different output power of a multiwave LED LCU on the degree of conversion and microhardness of a pit and fissure sealant comparing a 1000 mW/cm^2 curing mode to 1400 mW/cm^2 and 3200 mW/cm^2 curing modes of the LED LCU using manufacturer's guidelines for curing times at 2, 4 and 6 mm distances.

SPECIFIC AIMS

1. Determine the amount of radiant exposure and irradiance delivered on the top and bottom surfaces of the resin-based pit and fissure sealant samples using the 1000 mW/cm^2, 1400 mW/cm^2 and 3200 mW/cm^2 curing modes of the LED LCU and the manufacturer's guidelines for curing times at 2, 4 and 6 mm distances.
2. Determine the degree of conversion percentage of a resin-based pit and fissure sealant using the 1000 mW/cm^2, 1400 mW/cm^2 and 3200 mW/cm^2 curing modes of the LED LCU and the manufacturer's guidelines for curing times at 2, 4 and 6 mm distances.
3. Determine the microhardness of a resin-based pit and fissure sealant using the 1000 mW/cm^2, 1400 mW/cm^2 and 3200 mW/cm^2 curing modes of the LED LCU and the manufacturer's guidelines for curing times at 2, 4 and 6 mm distances.

HYPOTHESES

Null hypotheses

1. The radiant exposure and irradiance delivered to the bottom of a resin-based pit and fissure sealant specimens using 1400 mW/cm^2 and 3200 mW/cm^2 curing modes will not demonstrate significant differences compared to the 1000 mW/cm^2 curing mode using manufacturer's guidelines for curing times at 2, 4 and 6 mm distances.
2. The degree of conversion of a resin-based pit and fissure sealant using 1400 mW/cm^2 and 3200 mW/cm^2 curing modes will not demonstrate significant differences compared to the 1000 mW/cm^2 curing mode using manufacturer's guidelines for curing times at 2, 4 and 6 mm distances.

3. The microhardness of a resin-based pit and fissure sealant using 1400 mW/cm^2 and 3200 mW/cm^2 curing modes will not demonstrate significant differences compared to the 1000 mW/cm^2 curing mode using manufacturer's guidelines for curing times at 2, 4 and 6 mm distances.

Alternative hypotheses

1. The radiant exposure and irradiance delivered to the bottom surfaces of a resin-based pit and fissure sealant specimens using 1400 mW/cm^2 and 3200 mW/cm^2 curing modes will significantly increase compared to the 1000 mW/cm^2 curing mode with increasing the curing time and decreasing the distance.
2. The degree of conversion of a resin-based pit and fissure sealant using 1400 mW/cm^2 and 3200 mW/cm^2 curing modes will significantly increase compared to the 1000 mW/cm^2 curing mode with increasing the curing time and decreasing the distance.
3. The microhardness of a resin-based pit and fissure sealant using 1400 mW/cm^2 and 3200 mW/cm^2 curing modes will significantly increase compared to the 1000 mW/cm^2 curing mode with increasing the curing time and decreasing the distance.

MATERIALS AND METHODS

This laboratory study was carried out using an opaque resin-based pit and fissure sealant (Delton Light Curing Sealant Direct Delivery System, DENTSPLY, York, PA).
A multiwave LED light curing unit (VALO, Ultradent, South, Utah) utilized and was evaluated on three different curing modes: Standard (S) (1000 mW/cm^2), High Power Plus (H) (1400 mW/cm^2) and Xtra Power (X) (3200 mW/cm^2). Table-1.

SPECIMEN PREPARATION

A total of 90-disc specimens were prepared using a Delrin mold (6 mm x 1 mm) (Figure-1) and divided into eighteen groups (n=5/group). Following manufacturer's guidelines of curing times, each mode had two curing times; the shortest curing time and the extended curing time. Each curing mode was used for the shortest and extended curing times at 2, 4, or 6 mm distance between the light guide and the top of the specimen (Table-2). The mechanical arm of a Managing Accurate Resin Curing System-Resin Calibrator (MARC-RC by Blue light Analytics Inc., Halifax, Canada) (Figure-2) was used as a mounting tool to maintain the LCU in a consistent position and distance during the specimens' light curing. The LCU light guide tip (9.6 mm in diameter) was centrally mounted and perpendicular to the MARC-RC sensors and the top surface of the specimens (Fgure-3). Equal markings were inscribed on four corners of the mold in order to standardize the placement of the specimen on the bottom MARC-RC sensor (Figure-4). The fissure sealant was injected into the mold with a Mylar strip under the mold to create a smooth surface. Every specimen was positioned over the 4-mm diameter MARC-RC bottom sensor to measure the amount of mean value of light irradiance transmitted to the bottom surface of the specimen during the duration of the exposure. Specimens were prepared in a controlled-orange ambient lit room with a room temperature of 70 °F (±1°) and a humidity of 24% (± 5%).

The value of light irradiance of the LED LCU was assessed via the 4-mm diameter top sensor of the MARC-RC every time before testing, to ensure the irradiance and radiant exposure generated from the LCU and applied on the top surface of the specimens were standardized throughout the study. The irradiance and radiant exposure at the bottom surfaces of specimens were collected during specimen light curing via the MARC-RC bottom sensor.

After the specimens were light cured, they were kept in the Delrin mold to standardize the degree of conversion (DC) and microhardness (KHN) measurements using the markings on the mold. All specimens were stored in a container and wrapped with a water wetted paper towel. The containers were stored in the dark under 100% relative humidity at 37°C for 24 hours. After 24 hours the DC test was performed. After the DC tests were completed, the KHN microhardness test was conducted group by group.

DEGREE OF CONVERSION TEST (DC)

The DC of the fissure sealant was assessed utilizing attenuated total reflection Fourier transform infrared (ATR-FTIR) spectroscopy (JASCO 4100 International Co., Tokyo, Japan) on a 1.8 mm round Diamond crystal disc (ATR-MIRacle^{TM}, Pike Technologies, Madison, WI, USA). The absorbance value was calculated using 64 scans and 4 cm^{-1} resolution. Three non-cured fissure sealant specimens were tested on the diamond crystal disk and clamped with a swivel pressure clamp to insure the proper adaptability. With regard to the cured specimens, three standardized non-overlapping measurements of the top and bottom surfaces were calculated; one for the upper half, one for the lower right side, and one for the lower left side. A swivel pressure clamp was used to secure the cured specimens to the diamond plate. The area under the curves (at 1607 and 1637 cm^{-1}) of uncured and cured pit and fissure sealant were employed to determine the DC percent according to the following equation:

$$\text{Degree of conversion} = \left(1 - \frac{\text{cured (area under 1637/area under 1607)}}{\text{uncured (area under 1637/area under 1607)}}\right) \times 100$$

The average DC values were calculated for each surface.

KNOOP MICROHARDNESS

In order to perform the KHN test, five indentations (Figure-5) were made at five different locations, at the upper, lower, right, left and center of the specimen with 1 mm distance between each indent and 2 mm away from the edges of each surface using a hardness tester (Leco LM247AT, MI, USA, software; Confident V 2.5.2). The mold markings were used to standardize the locations of the indents. The indentations were performed with a diamond indenter using a 25-

gram load and a 10-second dwell time. The average KHN values were calculated for each surface.

STATISTICAL ANALYSIS

The effects of curing mode, distance, and curing time on degree of conversion and microhardness were analyzed using 3-way ANOVA, with all 2-way and 3-way interactions included in the models. ANOVAs used to analyze radiant exposure and irradiance included an additional factor for top or bottom surface, and also included a random effect to correlate the top and bottom surfaces within a specimen. Pair-wise comparisons were made using Fisher's Protected Least Significant Differences. The distributions of the measurements were examined and a transformation of the data or nonparametric tests were used if needed. A 5% significance level was used for all tests. The effects of mode, distance, and time on each outcome were analyzed using ANOVA. Due to non-normal distributions, all outcomes were log-transformed before comparisons. A two-sided 5% significance level was used for all tests. The correlations between Knoop hardness values and DOC, using the top, bottom, and average of top and bottom were also calculated. Analyses were performed using SAS version 9.4 (SAS Institute, Inc., Cary, NC, USA).

SAMPLE SIZE JUSTIFICATION

With a sample size of 5 specimens per group, the study had 80% power to detect an effect size of 2.0, based on a two-sample t-test calculation and a two-sided 5% significance level.

RESULTS

Irradiance, radiant exposure, degree of conversion, and microhardness results for Standard mode (S) were compared to High Power Plus (H) and Xtra Power (X) modes. The results were analyzed using ANOVA. Due to non-normal distributions, all outcomes were log-transformed before comparisons. A two-sided 0.05 significance level was used for all tests. Comparisons were statistically significant if the p-value was < 0.05.

STANDARD MODE RESULTS (S):

The results for top irradiance (mW/cm^2) are shown in Table-3. The irradiance at 2 mm curing distance for 10s curing time was 1145.52 and for 30s curing time the irradiance was 1491.38. The irradiance at 4 mm curing distance for 10s curing time was 1345.83 and for 30s curing time the irradiance was 1675.56. The irradiance at 6 mm curing distance for 10s curing time was 720.83 and for 30s curing time the irradiance was 670.90.

The results for bottom irradiance (mW/cm^2) are shown in Table-4. The irradiance at 2 mm curing distance for 10s curing time was 63.24 and for 30s curing time the irradiance was 85.35. The irradiance at 4 mm curing distance for 10s curing time was 114.97 and for 30s curing time the irradiance was 62.04. The irradiance at 6 mm curing distance for 10s curing time was 44.22 and for 30s curing time the irradiance was 39.26.

The results for top radiant exposure (RE) (J/cm^2) are shown in Table-5.
RE at 2 mm curing distance for 10s curing time was 11.96 and for 30s curing time RE was 46.58.
RE at 4 mm curing distance for 10s curing time was 13.91 and for 30s curing time RE was 52.38.
RE at 6 mm curing distance for 10s curing time was 7.41 and for 30s curing time RE was 21.26.

The results for bottom radiant exposure (RE) (J/cm^2) are shown in Table-6.
RE at 2 mm curing distance for 10s curing time was 0.65 and for 30s curing time RE was 2.66.
RE at 4 mm curing distance for 10s curing time was 1.17 and for 30s curing time RE was 1.94.
RE at 6 mm curing distance for 10s curing time was 0.45 and for 30s curing time RE was 1.23.

The results for degree of conversion (DC) (%) for the top surfaces are shown in Table-7. DC at 2 mm curing distance for 10s curing time was 53.68 and for 30s curing time the radiant

exposure was 92.83. DC at 4 mm curing distance for 10s curing time was 69.50 and for 30s curing time DC was 91.69. DC at 6 mm curing distance for 10s curing time was 47.97 and for 30s curing time DC was 84.14.

The results for degree of conversion (DC) (%) for the bottom surfaces are shown in Table-8. DC at 2 mm curing distance for 10s curing time was 28.47 and for 30s curing time DC was 39.58. DC at 4 mm curing distance for 10s curing time was 31.38 and for 30s curing time DC was 45.33. DC at 6 mm curing distance for 10s curing time was 28.02 and for 30s curing time DC was 37.05.

The results for degree of conversion (DC) (%) for the average top and bottom surfaces are shown in Table-9. DC at 2 mm curing distance for 10s curing time was 41.07 and for 30s curing time DC was 66.21. DC at 4 mm curing distance for 10s curing time was 50.44 and for 30s curing time DC was 68.51. DC at 6 mm curing distance for 10s curing time was 37.99 and for 30s curing time DC was 60.60.

The results for Knoop Microhardness test (KHN) for the top surfaces are shown in Table-10. KHN at 2 mm curing distance for 10s curing time was 24.48 and for 30s curing time KHN was 31.08. KHN at 4 mm curing distance for 10s curing time was 25.76 and for 30s curing time KHN was 15.36. KHN at 6 mm curing distance for 10s curing time was 12.84 and for 30s curing time KHN was 51.16.

The results for Knoop Microhardness test (KHN) for the bottom surfaces are shown in Table-11. KHN at 2 mm curing distance for 10s curing time was 9.12 and for 30s curing time KHN was 28.20. KHN at 4 mm curing distance for 10s curing time was 18.00 and for 30s curing time KHN was 19.96. KHN at 6 mm curing distance for 10s curing time was 5.48 and for 30s curing time KHN was 13.96.

HIGH POWER PLUS MODE RESULTS (H):

H mode top irradiance levels were significantly higher than S mode at all distances when used with shortest curing times. H2-20 and H4-20 top irradiance levels were significantly lower than

S2-30 and S4-30 subsequently but no significant difference found between H6-20 and S6-30 (Table-3).

H2-8 bottom irradiance was significantly higher than S2-10 and H4-8 significantly lower than S4-10 but no significant difference found between H6-8 and S6-10. H4-20 and H6-20 were significantly higher than S4-30 and S6-30 subsequently but no significant difference found between H2-20 and S2-30 (Table-4).

H mode top RE levels were significantly higher than S mode at all distances when used with shortest curing times. H2-20 and H4-20 top RE levels were significantly lower than S2-30 and S4-30 subsequently but no significant difference found between H6-20 and S6-30 (Table-5).

H2-8 bottom RE was significantly higher than S2-10 and H4-8 was significantly lower than S4-10 but no significant difference found between H6-8 and S6-10. H4-20 and H6-20 were significantly higher than S4-30 and S6-30 subsequently but no significant difference found between H2-20 and S2-30 (Table-6).

For top surfaces H2-8 and H4-8 DC were significantly higher than S2-10 and S4-10 subsequently but no significant difference found between H6-8 and S6-10. H2-20 was significantly lower than S2-30 but no significant difference found between H4-20, H6-20 and S4-30, S6-30 (Table-7).

For bottom surfaces H2-8 DC was significantly higher than S2-10 but no significant difference found between H4-8, H6-8 and S4-10, S6-10. H4-20, H-6-20 were significantly lower than S4-30 and S6-30 but no significant difference found between H2-20 and S2-30 (Table-8).

For the average top and bottom surfaces H2-8 DC and H4-8 DC were significantly higher than S2-10 and S4-10 subsequently but no significant difference found between H6-8 and S6-10. H4-20, H-6-20 were significantly lower than S4-30 and S6-30 but no significant difference found between H2-20 and S2-30 (Table-9).

H2-8 KHN at top surface was significantly lower than S2-10 but no significant difference found between H4-8, H6-8 and S4-10, S6-10. H2-20, H6-20 was significantly lower than S2-30 and S6-30 subsequently but no significant difference found between H4-20 and S4-30 (Table-10).

H2-8 KHN at bottom surface was significantly higher than S2-10 but H4-8 and H6-8 were significantly lower than S4-10 and S6-10 subsequently. H2-20 was significantly lower than S2-30 but H4-20 and H6-20 were significantly higher than S4-30 and S6-30 subsequently (Table-11).

XTRA POWER MODE RESULTS (X):

X mode top irradiance levels were significantly higher than S mode at all curing distances using both shortest and extended curing times (Table-3).

X2-3 and X6-3 bottom irradiances were significantly higher than S2-10 and S6-10 but no significant difference found between X4-3 and S4-10. X mode bottom irradiances were significantly higher than S mode bottom irradiances when used for extended curing times at all curing distances (Table-4).

X2-3 and X4-3 top RE were significantly lower than S2-10 and S4-10 RE levels subsequently but no significant difference found between X6-3 and S6-10. X2- 9 and X4-9 top RE were significantly lower than S2-30 and S4-130 RE levels subsequently but no significant difference found between X6-3 and S6-10 (Table-5).

X4-3 bottom RE was significantly higher than S4-10 and X6-3 was significantly lower than S6-10 but no significance difference found between X2-3 and S2-10. There was no significant difference at all curing distances on the bottom RE between X and S modes when used for extended curing times (Table-6).

For top surfaces X mode DC values were significantly lower than S mode DC values all curing distances when used for shortest curing times. There was no significant difference at all curing distances on the top DC between X and S modes when used for extended curing times (Table-7).

For bottom surfaces X mode DC values were significantly higher than S mode DC values at all curing distances when used for shortest curing times. There was no significant difference at all curing distances between X mode and S mode bottom DC values when used for extended curing times (Table-8).

For the average top and bottom surfaces X4-9 and X6-3 DC were significantly lower than S4-30 and S6-10 DC values subsequently but no significant difference found between X and S mode DC values at any other curing times and distances (Table-9).

X mode KHN values at top surface were significantly lower than S mode at all curing distances when used for shortest curing times. X6-9 KHN was significantly lower than S6-30 curing distances but no significant difference found between X2-9, X4-9 and S2-30, S4-30 subsequently (Table-10).

X2-3 and X4-3 KHN at bottom surfaces were significantly lower than S2-10 and S4-10 subsequently but no significant difference was found between X6-3 and S6-10. There was no significant difference at all curing distances between X mode and S mode bottom KHN values (Table-11).

THE CORRELATIONS BETWEEN KNOOP HARDNESS AND DEGREE OF CONVERSION:

The correlations between Knoop hardness values and DOC, using the top, bottom, and average of top and bottom are presented in Table-12. The correlation between KHN and DOC for top surfaces was a positive correlation of 0.76 with p-value (<0.001). The correlation between KHN and DOC for bottom surfaces was a negative correlation of -0.04 with p-value (0.738). The correlation between KHN and DOC for the average top and bottom surfaces was a positive correlation of 0.60 with p-value (<0.001).

TABLES AND FIGURES

TABLE-1
Details of the composition of resin-based sealant and light-curing unit used in the study as described by the manufacturers.

Material/unit	Product name (manufacturer)	Composition
Pits and fissures sealant	Delton Light Curing Sealant Direct Delivery System, DENTSPLY, York, PA	Aromatic an alphatic dimethacrylate monomers Titanium Dioxide (opaque) Silicon Dioxide (opaque) Ethyl p-dimethylaminobenzoate (Initiator)
Light Curing Unit	Multiple emission peak LED LCU (VALO, Ultradent, South, Utah)	Wavelength Range: 385–515nm Irradiance: Standard Power: 1000mW/cm2 High Power: 1400mW/cm2 Xtra Power: 3200mW/cm2

TABLE-2
Tested groups identified by curing mode, distance and time.

LED LCU Mode	Standard (1000 mW/cm^2)			High Power Plus (1400 mW/cm^2)			Xtra Power (3200 mW/cm^2)		
Distance (mm)	2	4	6	2	4	6	2	4	6
Groups	S2-10	S4-10	S6-10	H2-8	H4-8	H6-8	X2-3	X4-3	X6-3
	S2-30	S4-30	S6-30	H2-20	H4-20	H6-20	X2-9	X4-9	X6-9

TABLE-3
Mean (standard deviation) irradiance values (mW/cm2) of the top surface for each light curing mode at the different light curing distances and curing times.

Standard			High Power Plus			Xtra Power		
2mm	4mm	6mm	2mm	4mm	6mm	2mm	4mm	6mm
S2-10	S4-10	S6-10	H2-8	H4-8	H6-8	X2-3	X4-3	X6-3
1145.52 ^{Ab*} (19.61)	1345.83 ^{Aa*} (2.68)	720.83 ^{Ac*} (3.95)	1946.89 ^{Aa*} (2.41)	1656.55 ^{Ab*} (5.30)	912.57 ^{Ac*} (2.16)	1939.77 ^{Aa*} (3.69)	1812.59 ^{Ab*} (7.35)	2166.54 ^{Ac*} (4.54)
S2-30	S4-30	S6-30	H2-20	H4-20	H6-20	X2-9	X4-9	X6-9
1491.38 ^{Bb*} (4.18)	1675.56 ^{Ba*} (20.45)	670.90 ^{Bc*} (3.11)	1446.39 ^{Bb*} (6.78)	1589.18 ^{Ba*} (5.25)	1008.80 ^{Bc*} (1.71)	2320.89 ^{Ba*} (14.93)	2038.04 ^{Bb*} (5.87)	1471.40 ^{Bc*} (42.10)

Different lowercase letters in each row and uppercase letters in each column indicate statistically significant differences in each LCU mode. *represents significantly different values between LCU modes at the specific time and distance.

TABLE-4

Mean (standard deviation) irradiance values (mW/cm^2) of the bottom surface for each light curing mode at the different light curing distances and curing times.

Standard			High Power Plus			Xtra Power		
2mm	4mm	6mm	2mm	4mm	6mm	2mm	4mm	6mm
S2-10	S4-10	S6-10	H2-8	H4-8	H6-8	X2-3	X4-3	X6-3
63.24 ^{Aa*} (11.19)	114.97 ^{Ab*} (40.83)	44.22 ^{Ac} (4.79)	201.98 ^{Aa*} (94.65)	72.27 ^{Ab*} (12.42)	44.80 $^{Ac\wedge}$ (5.92)	168.85 ^{Aa*} (58.67)	93.03 ^{Ab} (17.42)	181.67 $^{Aa*\wedge}$ (22.46)
S2-30	S4-30	S6-30	H2-20	H4-20	H6-20	X2-9	X4-9	X6-9
85.35 ^{Aa} (17.78)	62.04 ^{Bb*} (10.27)	39.26 ^{Ab*} (21.48)	73.33 $^{Ba\wedge}$ (17.61)	107.93 ^{Bb*} (26.34)	95.60 ^{Bb*} (9.18)	174.84 $^{Aa*\wedge}$ (81.02)	141.12 ^{Aa*} (55.07)	87.20 ^{Bb*} (29.59)

Different lowercase letters in each row and uppercase letters in each column indicate statistically significant differences in each LCU mode. */^ represents significantly different values between LCU modes at the specific time and distance.

TABLE-5

Mean (standard deviation) for the radiant exposure values of the top surface of the resin-based sealants cured by each light curing mode explored at the different curing distances and curing times.

Standard			High Power Plus			Xtra Power		
2mm	4mm	6mm	2mm	4mm	6mm	2mm	4mm	6mm
S2-10	S4-10	S6-10	H2-8	H4-8	H6-8	X2-3	X4-3	X6-3
11.96 ^{Aa*} (1.03)	13.91 ^{Ab*} (0.21)	7.41 ^{Ac*} (0.03)	18.77 $^{Aa*\wedge}$ (0.16)	15.50 $^{Ab*\wedge}$ (0.66)	8.54 $^{Ac*\wedge}$ (0.10)	6.46 $^{Aa*\wedge}$ (0.03)	6.05 $^{Ab*\wedge}$ (0.16)	7.30 $^{Ac\wedge}$ (0.15)
S2-30	S4-30	S6-30	H2-20	H4-20	H6-20	X2-9	X4-9	X6-9

46.58 ^{Ba*} (0.27)	52.38 ^{Bb*} (1.54)	21.26 ^{Bc*} (0.79)	34.15 ^{Ba*} (1.28)	36.65 $^{Bb*\wedge}$ (0.36)	25.26 $^{Bc*\wedge}$ (0.21)	34.12 ^{Ba*} (0.18)	30.85 $^{Bb*\wedge}$ (0.17)	21.55 $^{Bc\wedge}$ (0.06)

Different lowercase letters in each row and uppercase letters in each column indicate statistically significant differences in each LCU mode. */^ represents significantly different values between LCU modes at the specific time and distance.

TABLE-6

Mean (standard deviation) for the radiant exposure values of the bottom surface of the resin-based sealants cured by each light curing mode explored at the different curing distances and curing times.

Standard			High Power Plus			Xtra Power		
2mm	4mm	6mm	2mm	4mm	6mm	2mm	4mm	6mm
S2-10	S4-10	S6-10	H2-8	H4-8	H6-8	X2-3	X4-3	X6-3
0.65 ^{Aa*} (0.13)	1.17 ^{Ab*} (0.42)	0.45 ^{Ac} (0.05)	1.73 $^{Aa*\wedge}$ (0.75)	0.68 $^{Ab*\wedge}$ (0.08)	0.40 $^{Ac*\wedge}$ (0.05)	0.55 $^{Aa\wedge}$ (0.19)	0.30 $^{Ab*\wedge}$ (0.06)	0.59 $^{Aa*\wedge}$ (0.07)
S2-30	S4-30	S6-30	H2-20	H4-20	H6-20	X2-9	X4-9	X6-9
2.66 ^{Ba*} (0.55)	1.94 ^{Bab} (0.33)	1.23 ^{Bc*} (0.68)	1.72 ^{Aa*} (0.40)	2.65 ^{Bb} (0.66)	2.32 $^{Ba*\wedge}$ (0.22)	2.60 ^{Ba} (1.22)	1.99 ^{Bac} (0.94)	1.27 $^{Bbc\wedge}$ (0.41)

Different lowercase letters in each row and uppercase letters in each column indicate statistically significant differences in each LCU mode. */^ represents significantly different values between LCU modes at the specific time and distance.

TABLE-7

Mean (standard deviation) for the degree of conversion values of the top surface of the resin-based sealants cured by each light curing mode explored at the different curing distances and curing times.

Standard			High Power Plus			Xtra Power		
2mm	4mm	6mm	2mm	4mm	6mm	2mm	4mm	6mm
S2-10	S4-10	S6-10	H2-8	H4-8	H6-8	X2-3	X4-3	X6-3
53.68 ^{Ab*} (3.30)	69.50 ^{Aa*} (5.52)	47.97 ^{Ac} (2.86)	74.31 ^{Aa*} (6.32)	77.28 ^{Aa*} (1.86)	48.23 $^{Ab\wedge}$ (6.34)	32.63 ^{Aa*} (2.05)	38.15 ^{Ab*} (2.65)	14.04 $^{Ac*\wedge}$ (2.67)
S2-30	S4-30	S6-30	H2-20	H4-20	H6-20	X2-9	X4-9	X6-9
92.83 ^{Ba*} (1.87)	91.69 ^{Bac} (1.09)	84.14 ^{Bbc} (6.51)	82.29 ^{Aa*} (6.82)	88.12 ^{Aa} (10.56)	85.72 ^{Ba} (5.59)	89.56 ^{Ba} (7.13)	83.58 ^{Ba} (7.85)	82.48 ^{Ba} (7.71)

Different lowercase letters in each row and uppercase letters in each column indicate statistically significant differences in each LCU mode. */^ represents significantly different values between LCU modes at the specific time and distance.

TABLE-8

Mean (standard deviation) for the degree of conversion values of the bottom surface of the resin-based sealants cured by each light curing mode explored at the different curing distances and curing times.

Standard			High Power Plus			Xtra Power		
2mm	4mm	6mm	2mm	4mm	6mm	2mm	4mm	6mm
S2-10	S4-10	S6-10	H2-8	H4-8	H6-8	X2-3	X4-3	X6-3
28.47 ^{Aa*} (8.19)	31.38 ^{Aa} (8.42)	28.02 ^{Aa} (6.17)	62.90 ^{Aa*} (5.13)	42.30 ^{Ab} (5.96)	24.70 $^{Ac\wedge}$ (6.98)	53.78 ^{Aa*} (8.53)	54.30 ^{Aa*} (9.37)	37.73 $^{Ab*\wedge}$ (6.01)
S2-30	S4-30	S6-30	H2-20	H4-20	H6-20	X2-9	X4-9	X6-9
39.58 ^{Aa} (9.74)	45.33 ^{Bab*} (4.07)	37.05 ^{Bac*} (6.32)	37.50 ^{Ba} (11.59)	25.74 $^{Ba*\wedge}$ (7.57)	23.47 $^{Aa*\wedge}$ (8.05)	43.57 ^{Aa} (4.90)	39.28 $^{Ba\wedge}$ (6.17)	42.71 $^{Aa\wedge}$ (4.19)

Different lowercase letters in each row and uppercase letters in each column indicate statistically significant differences in each LCU mode. */^ represents significantly different values between LCU modes at the specific time and distance.

TABLE-9

Mean (standard deviation) for the degree of conversion values of the average top and bottom surfaces of the resin-based sealants cured by each light curing mode explored at the different curing distances and curing times.

Standard			High Power Plus			Xtra Power		
2mm	4mm	6mm	2mm	4mm	6mm	2mm	4mm	6mm
S2-10	S4-10	S6-10	H2-8	H4-8	H6-8	X2-3	X4-3	X6-3
41.07 ^{Aa*} (4.20)	50.44 ^{Aab*} (2.20)	37.99 ^{Aac*} (2.20)	68.61 ^{Aa*} (2.47)	59.79 ^{Ab*} (2.84)	36.46 ^{Ac*} (5.92)	43.21 ^{Aa*} (3.71)	46.23 ^{Aa*} (4.42)	25.89 ^{Ab*} (3.47)
S2-30	S4-30	S6-30	H2-20	H4-20	H6-20	X2-9	X4-9	X6-9
66.21 ^{Ba*} (5.01)	68.51 ^{Bab*} (1.98)	60.60 ^{Bac*} (2.88)	59.90 ^{Ba*} (5.36)	56.93 ^{Ba*} (1.98)	54.60 ^{Ba*} (4.55)	66.56 ^{Ba*} (4.78)	61.43 ^{Ba} (4.86)	62.60 ^{Ba*} (3.55)

Different lowercase letters in each row and uppercase letters in each column indicate statistically significant differences in each LCU mode. *represents significantly different values between LCU modes at the specific time and distance.

TABLE-10

Mean (standard deviation) for the Knoop hardness values of the top surface of the resin-based sealants cured by each light curing mode explored at the different curing distances and curing times.

Standard			High Power Plus			Xtra Power		
2mm	4mm	6mm	2mm	4mm	6mm	2mm	4mm	6mm
S2-10	S4-10	S6-10	H2-8	H4-8	H6-8	X2-3	X4-3	X6-3
24.48 ^{Aa*} (7.61)	25.76 ^{Aab*} (5.87)	12.84 ^{Ac*} (2.30)	15.00 $^{Aa*\wedge}$ (5.14)	21.24 $^{Aa\wedge}$ (6.71)	15.00 $^{Aa\wedge}$ (2.71)	5.84 $^{Aa*\wedge}$ (1.77)	5.48 $^{Aa*\wedge}$ (1.48)	4.56 $^{Aa*\wedge}$ (0.22)
S2-30	S4-30	S6-30	H2-20	H4-20	H6-20	X2-9	X4-9	X6-9
31.08 ^{Aa*} (6.58)	15.36 ^{Bb*} (5.18)	51.16 ^{Ba*} (20.29)	21.04 $^{Aa*\wedge}$ (4.70)	32.56 ^{Bb*} (7.74)	24.48 ^{Ba*} (7.61)	33.28 $^{Ba\wedge}$ (10.61)	21.48 ^{Ba} (12.55)	21.24 ^{Bb*} (5.65)

Different lowercase letters in each row and uppercase letters in each column indicate statistically significant differences in each LCU mode. */^ represents significantly different values between LCU modes at the specific time and distance.

TABLE-11

Mean (standard deviation) for the Knoop hardness values of the bottom surface of the resin-based sealants cured by each light curing mode explored at the different curing distances and curing times.

Standard			High Power Plus			Xtra Power		
2mm	4mm	6mm	2mm	4mm	6mm	2mm	4mm	6mm
S2-10	S4-10	S6-10	H2-8	H4-8	H6-8	X2-3	X4-3	X6-3
9.12 ^{Aa*} (1.73)	18.00 ^{Ab*} (5.87)	5.48 ^{Ac*} (0.46)	13.36 $^{Aa*\wedge}$ (5.14)	8.68 $^{Ab*\wedge}$ (6.71)	4.56 ^{Ac*} (2.71)	6.00 $^{Aa*\wedge}$ (2.29)	5.20 $^{Aa*\wedge}$ (0.45)	5.04 ^{Aa} (0.46)
S2-30	S4-30	S6-30	H2-20	H4-20	H6-20	X2-9	X4-9	X6-9
28.20 ^{Ba*} (7.69)	19.96 ^{Bab*} (2.33)	13.96 ^{Bc*} (2.77)	17.88 $^{Ba*\wedge}$ (4.70)	25.44 ^{Bb*} (7.74)	24.92 $^{Ab*\wedge}$ (3.50)	27.80 $^{Aa\wedge}$ (5.79)	21.28 ^{Bb} (1.95)	16.40 $^{Ac\wedge}$ (2.36)

Different lowercase letters in each row and uppercase letters in each column indicate statistically significant differences in each LCU mode. */^ represents significantly different values between LCU modes at the specific time and distance.

TABLE-12

The correlations between Knoop hardness and DOC, using the top, bottom, and average of top and bottom.

	Correlation between Hardness and DOC		
	N	Correlation	p-value
Top	90	0.76	<.001
Bottom	90	-0.04	0.738
Average of Top and Bottom	90	0.60	<.001

FIGURE-1
Delrin mold design.

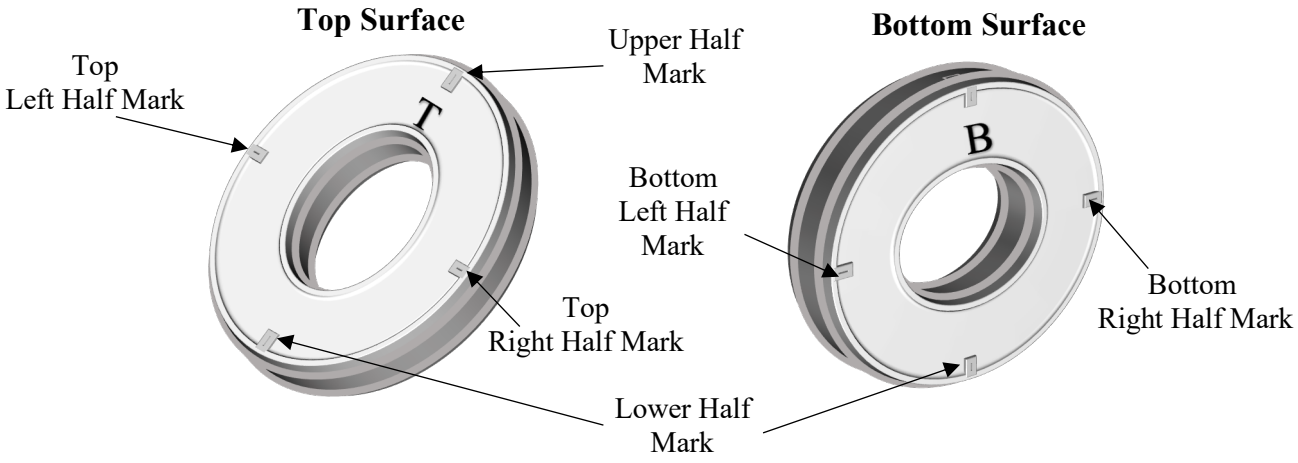

Delrin mold design that used to fabricate the samples. Markings on the mold performed to standardize the location of the sample when performing the DC and microhardness experiments.

FIGURE-2
LCU mounted on the MARC-RC.

FIGURE-3
LCU tip markings.

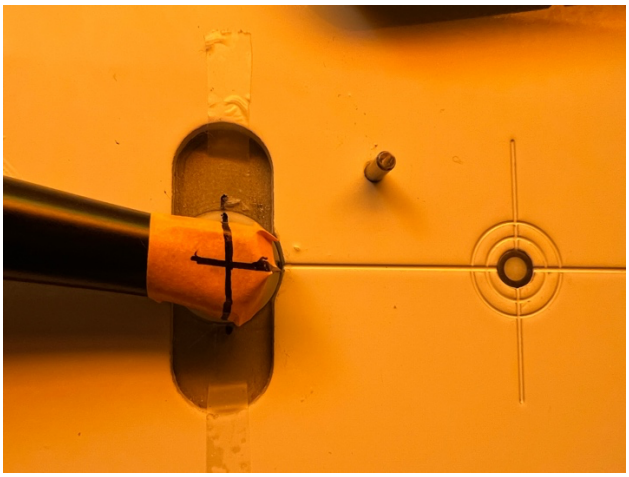

The LCU light guide tip (9.6 mm in diameter) was centrally mounted and perpendicular to the MARC-RC top, bottom sensors and the top surface of the specimens.

FIGURE-4
Delrin mold markings.

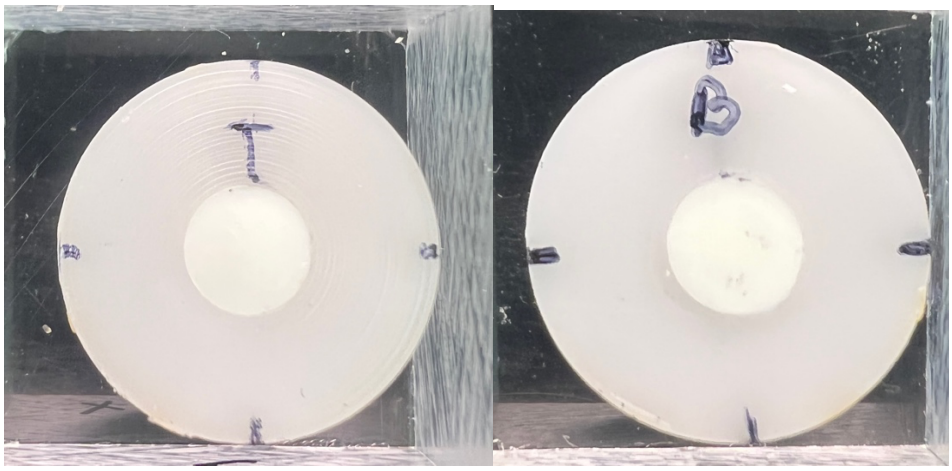

Markings have been inscribed on four corners of the mold in order to standardize the placement of the sample on bottom of the MARC-RC sensor.

FIGURE-5
Knoop Microhardness Indentations.

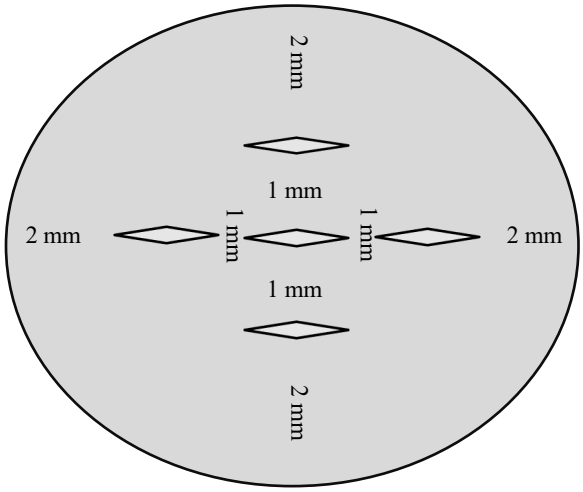

An illustration of the five indentations that have been performed on top and bottom surface of each sample, at the upper, lower, right, left and center of the specimen with 1 mm distance between each indent and 2 mm from edges.

DISCUSSION

This study assessed the effect of different settings of a multiwave LED LCU on the degree of conversion and microhardness of a pit and fissure sealant comparing 1000 mW/cm^2 curing mode to 1400 mW/cm^2 and 3200 mW/cm^2 curing modes of the LED LCU using manufacturer's guidelines for curing times at 2, 4 and 6 mm distances. All null hypotheses were partially rejected as results of this study showed some significant differences in means of irradiance, radiant exposure, degree of conversion, and Knoop microhardness in favor of Standard mode (S) over High (H) and Xtra (X) power modes at some curing times and curing distances but not others. In this study we tested each curing mode at two different curing times following manufacturer's guidelines of curing times for each mode, the first time was selected to resemble the curing of a one-layer resin material and the second time selected to resemble the curing of a one-layer resin material with a final cure step.

For resin-based sealants to perform successfully and to retain their integrity, an adequate depth of cure is imperative. As required by the International Organization for Standardization (ISO 6874), resin-based pit and fissure sealants that are light-cured must have a depth of cure of not less than 1.5 mm (109). The thickness of pit and fissure sealants generally does not exceed 1.5 mm under clinical conditions, but thicker layers may occur in deep fissures. It is possible to place the light tip of the curing unit at various distances from the sealant surface (110). The size and shape of the cusps and the morphology of the pits and fissures are primarily responsible for this, causing an increase in the dispersion of light and a diminution in the irradiance of the light that reaches the material (111). In order to mimic clinical conditions, the present study design had to consider both distance and sample thickness. In this present study, samples were kept in a dark environment at 37°C under 100% relative humidity for 24 hours in the incubator in order to reproduce clinically applicable settings, since heat energy may lead to the decomposition of initiators into free radicals or the direct reactivity of monomers (112).

When placing fissure sealants, especially on pediatric patients, a short curing time can be advantageous. The present study examined the shortest curing times available for each curing mode of the LCU in order to evaluate the mechanical properties of the resin-based fissure sealant. As supported by a number of studies, the resin-based sealant material properties are

mainly influenced by radiant exposure (RE) (15, 16). The radiant exposure is influenced by irradiance and time. For that reason, prolonged curing times will result in higher RE that will result in higher mechanical properties as discussed by A. Catelan et al and A. Peutzfeldt et al. The results of this study showed the same findings. On each curing mode, increasing exposure times resulted in higher RE and better mechanical properties (113, 114).

Sufficient polymerization is imperative for the successful and long-term performance of pit and fissure sealants (22). To initiate the photopolymerization process and transform the monomers into a complex polymer structure an adequate light activation is required (35). The polymerization process of resin-based material activated by the absorption of light in a certain range of wavelength results in reaction with the reducer agent to create free radicals which lead to the polymerization of the resin (40). The type and amount of photoinitiators contained in the resin-based sealant used is not clearly mentioned. The manufacturers' data only mentioned ethyl-4-dimethylamino benzoate (EDAB) as an initiator but have not disclosed other initiator details. EDAB has an absorbance range of 250-380 nm with a peak at 313 nm (115). The LED LCU used in the current study has an emission peak in the range of 385-515nm that is slightly higher than EDAB absorbance range. Therefore, the emission absorbance gap between EDAB and the LCU could have impacted the current DC% levels. As the degree of conversion is affected, other mechanical properties, (55, 56), volumetric shrinkage (57), wear resistance (58), and monomer elution (59) are also impacted thereby declining the sealants' longevity.

The opacity of the resin sealant used in this experiment is related to the titanium oxide which is used as an opacifying agent in its composition. The presence of titanium oxide is likely to cause considerable refraction, scattering, and absorption of light energy, which may prevent the sealant from being thoroughly cured. Consequently, the polymerization reaction is lessened in an opaque sealant and the DC% and KHN of the fissure sealant material is lowered (116, 117). Yue et al in 2009 observed a greater depth of cure for Delton Clear than Delton Opaque regardless of the curing time or distance (118). Also a previous study by S. M. Lucey et al. reported DC values at the bottom surfaces of the resin sealant were significantly higher for Delton Clear compared with Delton Opaque (119).

Irradiance and radiant exposure levels were not always related to the resultant degree of conversion and Knoop hardness. In some of High Power Plus (H) groups IR and RE had significantly higher values compared with Standard groups (S) that reflected on DC and KHN. While other H groups had significantly lower bottom IR and RE compared with S groups that reflected on KHN values but opposed by %DC.

While IR and RE are usually corelated, this was not always the case for Xtra Power groups. Additionally, the resultant DC and KHN did not reflect the effect of IR an RE on the sealants when using Xtra Power. All these odd relations between IR and RE and the subsequent DC and KHN are present on each curing mode.

From the results of this study, we can summarize that H mode at 2 mm distance and 8s duration resulted in higher DC% than S mode at 10s for both top and bottom surface. On the other hand, at all curing distances X mode at 3s resulted in significantly lower DC% at top surfaces but significantly higher DC% at bottom surfaces than S mode at 10s.

As per current results, H mode at 2 mm distance and 8s duration resulted in lower KHN than S mode at 10s for top surfaces but higher KHN at bottom surfaces. While at all curing distances X mode at 3s resulted in significantly lower KHN at top surface and at 2 and 4mm for bottom surfaces.

According to our results, H mode at 2 mm distance and 20s duration resulted in lower DC% than S mode at 30s for top surface only. On the other hand, at all curing distances X mode at 9s resulted in comparable DC% at both top and bottom surfaces.

The H mode at 2 mm distance and 8s duration resulted in lower KHN than S mode at 10s for top surfaces but higher KHN at bottom surfaces. While at all curing distances X mode at 9s resulted in comparable KHN values but significantly lower KHN at top surface and at 6mm only.

The DC% at top surfaces for samples cured with Standard and High Power modes ranged from 48.23 to 92.83 and these values are appropriate and comparable with DC values reported on

previous studies regardless of curing time and distance. On the other hand, Xtra Power mode did not perform as well as other modes when used with shortest curing time at all distances and resulted in DC values that are less than 40% which are considered unacceptable. When X mode used for 9s, DC values were always over 82% which are excellent percentages (27-29).

The DC% at bottom surfaces for S mode when used with shortest curing times were comparable values reported by Alqahtani, et al (120) but not up to the desired values compared to top surfaces and values reported by Santini, et al (28). Interestingly Xtra Power mode when used with shortest curing time had higher DC values on bottom surfaces compared with top surfaces.

The average top and bottom surfaces DC values presented in Table-9. When used at shortest curing times and 6 mm curing distances the values were below 40% which are considered unacceptable. H mode when used on shortest curing time resulted on the highest DC% averages. The average top and bottom surfaces DC values for all curing modes when used for the extended curing times resulted on DC values of 54% which considered on the acceptable range.

In this present study, KHN values for top and bottom surfaces were within acceptable ranges and comparable with values reported by Bani et al and Alqhatani et al (120, 121). The only exception found with Xtra Power mode when used with shortest curing time at all distances. An indirect method to determine the degree of conversion is to calculate the ratio of bottom to top surface values. The ratios should not result in more than 20% difference between hardness values of top and bottom surfaces (19). A ratio of around 80% is supposed to indicate a high %DC. In this present study, this was not always the case, especially with Xtra Power when used on shortest curing time. The %DC for X mode was too low but the KHN ratios were more than 80%.

The results for the top irradiance (Table-3) and top Radiant Exposure (Table-5) measured each time before specimens light curing show a significant decrease in both irradiance and radiant exposure between top and bottom surface (Table-4 and 6). These findings represent how much light energy is lost from the actual levels emitted from the LCU to the top surface of the resin

material and how significantly these energies decrease during the light curing of the resin materials.

Microhardness measurements have been indirectly used to evaluate the DC as a good linear correlation has been observed between DC and microhardness values. A positive linear correlation of 0.60 was observed between DC and KHN average values in the present study (Table-12) that coincide with findings reported by Ferracane et al (63).

CONCLUSIONS

- Within the limitations of the present study, using a multiwave LED LCU to polymerize Delton Opaque resin-based fissure sealants will result in a optimal DC and KHN values for any irradiance level if the curing distance is kept at 4 mm or less and with at least three cycles of the shortest curing time recommended by manufacturers for all curing modes.
- Using a multiwave LED LCU with 1000, 1400 or 3200 mW/cm^2 irradiance levels with the shortest recommended curing times resulted in unsatisfactory DC and KHN levels.
- LED LCU with high and extra high irradiance levels (1400 and 3200 mW/cm^2) can result in high DC and KHN levels if the curing distance is kept at 4 mm or less and with at least three cycles of the shortest curing time recommended by manufacturers.
- Xtra Power mode (3200 mW/cm^2) used with the shortest curing time (3 seconds) resulted in significantly lower mechanical properties and for that reason it is not recommended to be used.
- High Power Plus (1400 mW/cm^2) when used for 20 seconds and Xtra Power (3200 mW/cm^2) when used for 9 seconds had sufficient mechanical properties that are comparable with those obtained with the Standard/ Control irradiance (1000 mW/cm^2) used for 30 seconds.
- Dentists planning to use the Valo Cordless LED LCU with increased level of irradiance higher than 1000 mW/cm^2 are advised to keep the curing distance less than 4 mm and to cure for at least 20 seconds with the High power mode and at least 9 seconds with the Xtra power mode.

REFERENCES

1. Ahovuo-Saloranta A, Forss H, Hiiri A, Nordblad A, Makela M. Pit and fissure sealants versus fluoride varnishes for preventing dental decay in the permanent teeth of children and adolescents. Cochrane Database Syst Rev. 2016(1):CD003067.
2. Simonsen RJ. Pit and fissure sealants. In: Clinical Applications of the Acid Etch Technique. 1st ed. Chicago, IL: Quintessence Publishing Co, Inc; 1978.
3. Soto-Rojas AE YK, Krushinski C, Eberhardt C, Maupome G. Comparison of Isolation Methods for Sealing Teeth in a Mobile Program. Caries Res. 2010;44:218
4. Imazato S, McCabe JF, Tarumi H, Ehara A, Ebisu S. Degree of conversion of composites measured by DTA and FTIR. Dent Mater. 2001;17(2):178-83.
5. Buonocore MG. A simple method of increasing the adhesion of acrylic filling materials to enamel surfaces. J Dent Res. 1955;34(6):849-53.
6. Simonsen RJ, Neal RC. A review of the clinical application and performance of pit and fissure sealants. Aust Dent J. 2011;56 Suppl 1:45-58.
7. Wright JT, Tampi MP, Graham L, Estrich C, Crall JJ, Fontana M, et al. Sealants for preventing and arresting pit-and-fissure occlusal caries in primary and permanent molars: A systematic review of randomized controlled trials-a report of the American Dental Association and the American Academy of Pediatric Dentistry. J Am Dent Assoc. 2016;147(8):631-45.e18.
8. Ripa LW. Sealants revisted: an update of the effectiveness of pit-and-fissure sealants. Caries Res. 1993;27 Suppl 1:77-82.
9. Carlsson A, Petersson M, Twetman S. 2-year clinical performance of a fluoride-containing fissure sealant in young schoolchildren at caries risk. Am J Dent. 1997;10(3):115-9.
10. de Oliveira DC, Rocha MG, Gatti A, Correr AB, Ferracane JL, Sinhoret MA. Effect of different photoinitiators and reducing agents on cure efficiency and color stability of resin-based composites using different LED wavelengths. J Dent. 2015;43(12):1565-72.
11. Santini A, Miletic V, Swift MD, Bradley M. Degree of conversion and microhardness of TPO-containing resin-based composites cured by polywave and monowave LED units. J Dent. 2012;40(7):577-84.
12. Mohammed A, Ario S. Resin-Based Composite and LCU-related Factors Affecting the Degree of Cure. A Literature Review: Part 2. Light Curing Units & Related Factors. Acta Medica Marisiensis. 2015;61:255 - 60.
13. Platt JA, Clark H, Moore BK. Curing of pit & fissure sealants using Light Emitting Diode curing units. Oper Dent. 2005;30(6):764-71.
14. Platt JA, Price RB. Light curing explored in Halifax. Oper Dent. 2014;39(6):561-3.
15. Manojlovic D, Radisic M, Vasiljevic T, Zivkovic S, Lausevic M, Miletic V. Monomer elution from nanohybrid and ormocer-based composites cured with different light sources. Dent Mater. 2011;27(4):371-8.
16. Turssi CP, Ferracane JL, Vogel K. Filler features and their effects on wear and degree of conversion of particulate dental resin composites. Biomaterials. 2005;26(24):4932-7.
17. Guiraldo RD, Consani S, Sinhoreti MA, Correr-Sobrinho L, Schneider LF. Thermal variations in the pulp chamber associated with composite insertion techniques and light-curing methods. J Contemp Dent Pract. 2009;10(1):17-24.
18. Leprince J, Devaux J, Mullier T, Vreven J, Leloup G. Pulpal-temperature rise and polymerization efficiency of LED curing lights. Oper Dent. 2010;35(2):220-30.

19. Cassoni A, Ferla Jde O, Shibli JA, Kawano Y. Knoop microhardness and FT-Raman spectroscopic evaluation of a resin-based dental material light-cured by an argon ion laser and halogen lamp: an in vitro study. Photomed Laser Surg. 2008;26(6):531-9.
20. Eliades T, Eliades G, Brantley WA, Johnston WM. Residual monomer leaching from chemically cured and visible light-cured orthodontic adhesives. Am J Orthod Dentofacial Orthop. 1995;108(3):316-21.
21. Geurtsen W, Lehmann F, Spahl W, Leyhausen G. Cytotoxicity of 35 dental resin composite monomers/additives in permanent 3T3 and three human primary fibroblast cultures. J Biomed Mater Res. 1998;41(3):474-80.
22. Santini A. Current status of visible light activation units and the curing of light-activated resin-based composite materials. Dent Update. 2010;37(4):214-6, 8-20, 23-7.
23. Roydhouse RH. Prevention of occlusal fissure caries by use of a sealant: a pilot study. ASDC J Dent Child. 1968;35(3):253-62.
24. Czasch P, Ilie N. In vitro comparison of mechanical properties and degree of cure of bulk fill composites. Clin Oral Investig. 2013;17(1):227-35.
25. Smallridge J. UK National Clinical Guidelines in Paediatric Dentistry. Management of the stained fissure in the first permanent molar. Int J Paediatr Dent. 2000;10(1):79-83.
26. Yan YL, Kim YK, Kim KH, Kwon TY. Changes in degree of conversion and microhardness of dental resin cements. Oper Dent. 2010;35(2):203-10.
27. Kuşgöz A, Tüzüner T, Ulker M, Kemer B, Saray O. Conversion degree, microhardness, microleakage and fluoride release of different fissure sealants. J Mech Behav Biomed Mater. 2010;3(8):594-9.
28. Santini A, Miletic V, Koutsaki D. Degree of conversion of three fissure sealants cured by different light curing units using micro-Raman spectroscopy. Journal of Dental Sciences. 2012;7(1):26-32.
29. Osorio E, Osorio R, Davidenko N, Sastre R, Aguilar JA, Toledano M. Polymerization kinetics and mechanical characterization of new formulations of light-cured dental sealants. J Biomed Mater Res B Appl Biomater. 2007;80(1):18-24.
30. Ünal M, Oznurhan F, Kapdan A, Dürer S. A comparative clinical study of three fissure sealants on primary teeth: 24-month results. J Clin Pediatr Dent. 2015;39(2):113-9.
31. Zhang W, Chen X, Fan MW, Mulder J, Huysmans MC, Frencken JE. Do light cured ART conventional high-viscosity glass-ionomer sealants perform better than resin-composite sealants: a 4-year randomized clinical trial. Dent Mater. 2014;30(5):487-92.
32. Karaman E, Yazici AR, Tuncer D, Firat E, Unluer S, Baseren M. A 48-month clinical evaluation of fissure sealants placed with different adhesive systems. Oper Dent. 2013;38(4):369-75.
33. Fatima N. Influence of extended light exposure curing times on the degree of conversion of resin-based pit and fissure sealant materials. Saudi Dent J. 2014;26(4):151-5.
34. Branchal CF, Wells MH, Tantbirojn D, Versluis A. Can Increasing the Manufacturer's Recommended Shortest Curing Time of High-intensity Light-emitting Diodes Adequately Cure Sealants? Pediatr Dent. 2015;37(4):E7-13.
35. Kitchens B, Wells M, Tantbirojn D, Versluis A. Depth of cure of sealants polymerized with high-power light emitting diode curing lights. Int J Paediatr Dent. 2015;25(2):79-86.

36. Anusavice KJ SC, Rawls HR, Phillips RW. Phillips' Science of Dental Materials. St. Louis, MO: Elsevier; 2013.
37. Beauchamp J, Caufield PW, Crall JJ, Donly K, Feigal R, Gooch B, et al. Evidence-based clinical recommendations for the use of pit-and-fissure sealants: a report of the American Dental Association Council on Scientific Affairs. J Am Dent Assoc. 2008;139(3):257-68.
38. San-Martin L, Ogunbodede EO, Kalenderian E. A 50-year audit of published peer-reviewed literature on pit and fissure sealants, 1962-2011. Acta Odontol Scand. 2013;71(6):1356-61.
39. Rueggeberg FA, Giannini M, Arrais CAG, Price RBT. Light curing in dentistry and clinical implications: a literature review. Braz Oral Res. 2017;31(suppl 1):e61.
40. Asmussen E, Peutzfeldt A. Influence of specimen diameter on the relationship between subsurface depth and hardness of a light-cured resin composite. Eur J Oral Sci. 2003;111(6):543-6.
41. Stansbury JW, Dickens SH. Determination of double bond conversion in dental resins by near infrared spectroscopy. Dent Mater. 2001;17(1):71-9.
42. Obici AC, Sinhoreti MA, Correr Sobrinho L, de Goes MF, Consani S. Evaluation of depth of cure and Knoop hardness in a dental composite photo-activated using different methods. Braz Dent J. 2004;15(3):199-203.
43. Leprince JG, Palin WM, Hadis MA, Devaux J, Leloup G. Progress in dimethacrylate-based dental composite technology and curing efficiency. Dent Mater. 2013;29(2):139-56.
44. Arenholt-Bindslev GSaD. Resin-based composites. Biocompatibility of Dental Materials. 2009:99–137. Berlin/Heidelberg/Germany: Springer-Verlag; 2009.
45. Cramer NB, Stansbury JW, Bowman CN. Recent advances and developments in composite dental restorative materials. J Dent Res. 2011;90(4):402-16.
46. Anseth KS, Newman SM, Bowman CN. Polymeric dental composites : properties and reaction behavior of multimethacrylate dental restorations. Advances in Polymer Science. 1995;122:177-217.
47. Lovell LG, Stansbury JW, Syrpes DC, Bowman CN. Effects of Composition and Reactivity on the Reaction Kinetics of Dimethacrylate/Dimethacrylate Copolymerizations. Macromolecules. 1999;32(12):3913-21.
48. Ferracane JL. Current trends in dental composites. Crit Rev Oral Biol Med. 1995;6(4):302-18.
49. CLaa G. LED Technology Here to stay. 3m ESPE. 2002;2002:1-6.
50. Jandt KD, Mills RW. A brief history of LED photopolymerization. Dent Mater. 2013;29(6):605-17.
51. Christensen GJ. The curing light dilemma. J Am Dent Assoc. 2002;133(6):761-3.
52. Hofmann N, Hugo B, Klaiber B. Effect of irradiation type (LED or QTH) on photo-activated composite shrinkage strain kinetics, temperature rise, and hardness. Eur J Oral Sci. 2002;110(6):471-9.
53. Leonard DL, Charlton DG, Roberts HW, Cohen ME. Polymerization efficiency of LED curing lights. J Esthet Restor Dent. 2002;14(5):286-95.
54. Jandt KD, Mills RW, Blackwell GB, Ashworth SH. Depth of cure and compressive strength of dental composites cured with blue light emitting diodes (LEDs). Dent Mater. 2000;16(1):41-7.

55. Ferracane JL, Greener EH. The effect of resin formulation on the degree of conversion and mechanical properties of dental restorative resins. J Biomed Mater Res. 1986;20(1):121-31.
56. Truffier-Boutry D, Demoustier-Champagne S, Devaux J, Biebuyck JJ, Mestdagh M, Larbanois P, et al. A physico-chemical explanation of the post-polymerization shrinkage in dental resins. Dent Mater. 2006;22(5):405-12.
57. Li J, Li H, Fok AS, Watts DC. Multiple correlations of material parameters of light-cured dental composites. Dent Mater. 2009;25(7):829-36.
58. Dewaele M, Truffier-Boutry D, Devaux J, Leloup G. Volume contraction in photocured dental resins: the shrinkage-conversion relationship revisited. Dent Mater. 2006;22(4):359-65.
59. Ferracane JL. Elution of leachable components from composites. J Oral Rehabil. 1994;21(4):441-52.
60. Ferracane JL, Greener EH. Fourier transform infrared analysis of degree of polymerization in unfilled resins--methods comparison. J Dent Res. 1984;63(8):1093-5.
61. Pianelli C, Devaux J, Bebelman S, Leloup G. The micro-Raman spectroscopy, a useful tool to determine the degree of conversion of light-activated composite resins. J Biomed Mater Res. 1999;48(5):675-81.
62. Duangthip D, Ballungpattama S, Sitthisettapong T. Effect of light curing methods on microleakage and microhardness of different resin sealants. J Dent Child (Chic). 2011;78(2):88-95.
63. Ferracane JL. Correlation between hardness and degree of conversion during the setting reaction of unfilled dental restorative resins. Dent Mater. 1985;1(1):11-4.
64. Leprince JG, Leveque P, Nysten B, Gallez B, Devaux J, Leloup G. New insight into the "depth of cure" of dimethacrylate-based dental composites. Dent Mater. 2012;28(5):512-20.
65. Musanje L, Darvell BW. Curing-light attenuation in filled-resin restorative materials. Dent Mater. 2006;22(9):804-17.
66. Dewaele M, Asmussen E, Peutzfeldt A, Munksgaard EC, Benetti AR, Finné G, et al. Influence of curing protocol on selected properties of light-curing polymers: degree of conversion, volume contraction, elastic modulus, and glass transition temperature. Dent Mater. 2009;25(12):1576-84.
67. Palin WM, Fleming GJ, Marquis PM. The reliability of standardized flexure strength testing procedures for a light-activated resin-based composite. Dent Mater. 2005;21(10):911-9.
68. Ilie N, Hickel R, Watts DC. Spatial and cure-time distribution of dynamic-mechanical properties of a dimethacrylate nano-composite. Dent Mater. 2009;25(3):411-8.
69. Flury S, Hayoz S, Peutzfeldt A, Hüsler J, Lussi A. Depth of cure of resin composites: is the ISO 4049 method suitable for bulk fill materials? Dent Mater. 2012;28(5):521-8.
70. Cook WD. Photopolymerization kinetics of dimethacrylates using the camphorquinone/amine initiator system. Polymer. 1992;33(3):600-9.
71. Leprince J, Lamblin G, Truffier-Boutry D, Demoustier-Champagne S, Devaux J, Mestdagh M, et al. Kinetic study of free radicals trapped in dental resins stored in different environments. Acta Biomater. 2009;5(7):2518-24.
72. Jakubiak J, Allonas X, Fouassier JP, Sionkowska A, Andrzejewska E, Linden LÅ, et al. Camphorquinone–amines photoinitating systems for the initiation of free radical polymerization. Polymer. 2003;44(18):5219-26.

73. Musanje L, Ferracane JL, Sakaguchi RL. Determination of the optimal photoinitiator concentration in dental composites based on essential material properties. Dent Mater. 2009;25(8):994-1000.
74. Park J, Ye Q, Topp EM, Misra A, Kieweg SL, Spencer P. Effect of photoinitiator system and water content on dynamic mechanical properties of a light-cured bisGMA/HEMA dental resin. J Biomed Mater Res A. 2010;93(4):1245-51.
75. Pfeifer CS, Ferracane JL, Sakaguchi RL, Braga RR. Photoinitiator content in restorative composites: influence on degree of conversion, reaction kinetics, volumetric shrinkage and polymerization stress. Am J Dent. 2009;22(4):206-10.
76. Shin DH, Rawls HR. Degree of conversion and color stability of the light curing resin with new photoinitiator systems. Dent Mater. 2009;25(8):1030-8.
77. Cook WD, Chen F. Enhanced photopolymerization of dimethacrylates with ketones, amines, and iodonium salts: The CQ system. Journal of Polymer Science Part A: Polymer Chemistry. 2011;49(23):5030-41.
78. Lovell LG, Newman SM, Bowman CN. The effects of light intensity, temperature, and comonomer composition on the polymerization behavior of dimethacrylate dental resins. J Dent Res. 1999;78(8):1469-76.
79. Ogunyinka A, Palin WM, Shortall AC, Marquis PM. Photoinitiation chemistry affects light transmission and degree of conversion of curing experimental dental resin composites. Dent Mater. 2007;23(7):807-13.
80. Shortall AC, Wilson HJ, Harrington E. Depth of cure of radiation-activated composite restoratives--influence of shade and opacity. J Oral Rehabil. 1995;22(5):337-42.
81. Arikawa H, Kanie T, Fujii K, Takahashi H, Ban S. Effect of inhomogeneity of light from light curing units on the surface hardness of composite resin. Dent Mater J. 2008;27(1):21-8.
82. Watts DC, Cash AJ. Analysis of optical transmission by 400-500 nm visible light into aesthetic dental biomaterials. J Dent. 1994;22(2):112-7.
83. Chen YC, Ferracane JL, Prahl SA. Quantum yield of conversion of the photoinitiator camphorquinone. Dent Mater. 2007;23(6):655-64.
84. Craig RG. Chemistry, composition, and properties of composite resins. Dent Clin North Am. 1981;25(2):219-39.
85. Lienhard OE, inventor; Canrad Precision Industries, Inc. , assignee. INSTRUMENT FOR TRANSMITTING ULTRAVIOLET
RADIATION TO A LIMITED AREA. United States1973 Jan. 23, 1973
86. Stansbury JW. Curing dental resins and composites by photopolymerization. J Esthet Dent. 2000;12(6):300-8.
87. Tirtha R, Fan PL, Dennison JB, Powers JM. In vitro depth of cure of photo-activated composites. J Dent Res. 1982;61(10):1184-7.
88. Rueggeberg FA. State-of-the-art: dental photocuring--a review. Dent Mater. 2011;27(1):39-52.
89. Krämer N, Lohbauer U, García-Godoy F, Frankenberger R. Light curing of resin-based composites in the LED era. Am J Dent. 2008;21(3):135-42.
90. Price RB, Felix CA. Effect of delivering light in specific narrow bandwidths from 394 to 515nm on the micro-hardness of resin composites. Dent Mater. 2009;25(7):899-908.

91. Miyazaki M, Oshida Y, Moore BK, Onose H. Effect of light exposure on fracture toughness and flexural strength of light-cured composites. Dent Mater. 1996;12(6):328-32.
92. Nomoto R, McCabe JF, Nitta K, Hirano S. Relative efficiency of radiation sources for photopolymerization. Odontology. 2009;97(2):109-14.
93. Price RB, Fahey J, Felix CM. Knoop hardness of five composites cured with single-peak and polywave LED curing lights. Quintessence Int. 2010;41(10):e181-91.
94. Price RB, Felix CA, Andreou P. Effects of resin composite composition and irradiation distance on the performance of curing lights. Biomaterials. 2004;25(18):4465-77.
95. Price RB, Labrie D, Rueggeberg FA, Felix CM. Irradiance differences in the violet (405 nm) and blue (460 nm) spectral ranges among dental light-curing units. J Esthet Restor Dent. 2010;22(6):363-77.
96. Vandewalle KS. Commentary. Irradiance differences i n the violet (405 nm) and blue (460 nm) spectral ranges among dental light-curing units. J Esthet Restor Dent. 2010;22(6):378.
97. Vandewalle KS, Roberts HW, Rueggeberg FA. Power distribution across the face of different light guides and its effect on composite surface microhardness. J Esthet Restor Dent. 2008;20(2):108-17; discussion 18.
98. Price RB, Rueggeberg FA, Labrie D, Felix CM. Irradiance uniformity and distribution from dental light curing units. J Esthet Restor Dent. 2010;22(2):86-101.
99. Cunha LG, Alonso RC, Pfeifer CS, Correr-Sobrinho L, Ferracane JL, Sinhoreti MA. Contraction stress and physical properties development of a resin-based composite irradiated using modulated curing methods at two C-factor levels. Dent Mater. 2008;24(3):392-8.
100. Ilie N, Jelen E, Hickel R. Is the soft-start polymerisation concept still relevant for modern curing units? Clin Oral Investig. 2011;15(1):21-9.
101. Kanca J, 3rd, Suh BI. Pulse activation: reducing resin-based composite contraction stresses at the enamel cavosurface margins. Am J Dent. 1999;12(3):107-12.
102. Vandewalle KS, Roberts HW, Andrus JL, Dunn WJ. Effect of light dispersion of LED curing lights on resin composite polymerization. J Esthet Restor Dent. 2005;17(4):244-54; discussion 54-5.
103. Cunha LG, Alonso RC, Pfeifer CS, Correr-Sobrinho L, Ferracane JL, Sinhoreti MA. Modulated photoactivation methods: Influence on contraction stress, degree of conversion and push-out bond strength of composite restoratives. J Dent. 2007;35(4):318-24.
104. Price RB, Whalen JM, Price TB, Felix CM, Fahey J. The effect of specimen temperature on the polymerization of a resin-composite. Dent Mater. 2011;27(10):983-9.
105. Michaud PL, Price RB, Labrie D, Rueggeberg FA, Sullivan B. Localised irradiance distribution found in dental light curing units. J Dent. 2014;42(2):129-39.
106. Daronch M, Rueggeberg FA, De Goes MF, Giudici R. Polymerization kinetics of pre-heated composite. J Dent Res. 2006;85(1):38-43.
107. Price RB, Labrie D, Whalen JM, Felix CM. Effect of distance on irradiance and beam homogeneity from 4 light-emitting diode curing units. J Can Dent Assoc. 2011;77:b9.
108. Fróes-Salgado NR, Pfeifer CS, Francci CE, Kawano Y. Influence of photoactivation protocol and light guide distance on conversion and microleakage of composite restorations. Oper Dent. 2009;34(4):408-14.
109. Standardization IOf. ISO 6874:2015
Polymer-based pit and fissure sealants. Dentistry

1106010 - Dental materials: ISO; 2015.
110. Mills RW, Uhl A, Jandt KD. Optical power outputs, spectra and dental composite depths of cure, obtained with blue light emitting diode (LED) and halogen light curing units (LCUs). Br Dent J. 2002;193(8):459-63; discussion 5.
111. Borges BC, Bezerra GV, Mesquita Jde A, Pereira MR, Aguiar FH, Santos AJ, et al. Effect of irradiation times on the polymerization depth of contemporary fissure sealants with different opacities. Braz Oral Res. 2011;25(2):135-42.
112. Aspell C. Polymer science V. R. Gowariker, N. V. Viswanathan and Jayadev Sreedhar, Halsted Press (John Wiley & Sons), New York, 1986. pp. xv + 505, price £38.50. ISBN 0-470-20322-6. British Polymer Journal. 1988;20(1):88-.
113. Catelan A, Mainardi Mdo C, Soares GP, de Lima AF, Ambrosano GM, Lima DA, et al. Effect of light curing protocol on degree of conversion of composites. Acta Odontol Scand. 2014;72(8):898-902.
114. Peutzfeldt A, Asmussen E. Resin composite properties and energy density of light cure. J Dent Res. 2005;84(7):659-62.
115. Oliveira D, Ayres Oliveira AP, Rocha M, Giannini M, Puppin-Rontani R, Ferracane J, et al. Effect of Different In Vitro Aging Methods on Color Stability of a Dental Resin-Based Composite Using CIELAB and CIEDE2000 Color-Difference Formulas. 2016.
116. Shortall AC, Palin WM, Burtscher P. Refractive index mismatch and monomer reactivity influence composite curing depth. J Dent Res. 2008;87(1):84-8.
117. Zhu S, Platt J. Curing efficiency of three different curing modes at different distances for four composites. Oper Dent. 2011;36(4):362-71.
118. Yue C, Tantbirojn D, Grothe RL, Versluis A, Hodges JS, Feigal RJ. The depth of cure of clear versus opaque sealants as influenced by curing regimens. J Am Dent Assoc. 2009;140(3):331-8.
119. Lucey SM, Santini A, Roebuck EM. Degree of conversion of resin-based materials cured with dual-peak or single-peak LED light-curing units. Int J Paediatr Dent. 2015;25(2):93-102.
120. Alqahtani S, Al-Zain A, Platt J, Cook N, Soto-Rojas A. Effect of Multiple and Single Emission Peak Light Emitting Diode Light Curing Units on the Degree of Conversion and Microhardness of Resin-Based Pit and Fissure Sealant. EC Dental Science. 2017;14:157-66.
121. Bani M, Tirali RE. Effect of new light curing units on microleakage and microhardness of resin sealants. Dent Mater J. 2016;35(3):517-22.

ABSTRACT

Performance of Multiple Emission Peak Light Emitting Diode Light Curing Unit: Degree of Conversion and Microhardness of Resin-based Pit and Fissure Sealant

Background: The light-cured resin-based pit and fissure sealants success and longevity are enhanced by sufficient curing. Multiple emission peak Light Emitting Diode Light Curing Units offer a wider range of wavelengths and different levels of irradiances to ensure sufficient curing. The irradiance is considered a main curing factor that can affect the material properties.

Purpose: The aim of this study was to assess the effect of different settings of a multiwave LED LCU on the degree of conversion and microhardness of a pit and fissure sealant comparing the irradiance of 1000 mW/cm^2 to 1400 mW/cm^2 and 3200 mW/cm^2 irradiances of the LCU using manufacturer's guidelines for curing times at 2, 4 and, 6 mm distances.

Methods: A multiwave LED light curing unit was evaluated on three different irradiance levels 1000 mW/cm^2 (S), 1400 mW/cm^2 (H), and 3200 mW/cm^2 (X). A total of 90 samples made from the fissure sealant were fabricated and divided into eighteen groups (n=5/group). Samples were cured following manufacturer's guidelines of curing times for each curing mode at 2, 4, or 6 mm distance between the light tip and top of samples. The DC was measured using (ATR-FTIR) spectroscopy. The KHN test was performed on five different locations of each specimen using a hardness tester (Leco LM247AT, MI, USA, software; Confident V 2.5.2).

Results: The top DC for H-8 was significantly higher than S-10 at 2 and 4mm, H-20 DC was significantly lower than S-30 at only 2mm. The bottom DC for H-8 was significantly higher than S-10 at 2mm only, H-20 DC was significantly lower than S-30 at 4 and 6mm only. H-8 KHN at top surface was significantly lower than S-10 at 2mm only, H-20 was significantly lower than S-30 at 2 and 6mm only. H-8 KHN at bottom surface was significantly lower than S-10 at 4 and 6mm but significantly higher at 2mm. H-20 was significantly lower than S-30 at 2mm but significantly higher at 4 and 6mm. The top DC for X-3 was significantly lower than S-10 at all curing distances with no significant difference at all curing distances between X-9 and S-30. The bottom DC for X-3 was significantly higher than S-10 at all curing distances with no significant difference between X-9 and S-30. X-3 KHN at top surface was significantly lower than S-10s at all curing distances. X-9 was significantly lower than S-30 at 6mm only. X-3 KHN at bottom surface was significantly lower than S-10 at 2 and 4mm only with no significant difference at all curing distances between X-9 and S-30.

Conclusions: Using a multiwave LED LCU to polymerize Delton Opaque resin-based fissure sealants will result in an optimal DC and KHN values for any irradiance level if the curing distance is kept at 4 mm or less and with at least two cycles of the shortest curing time recommended by the manufacturer. Using a multiwave LED LCU with 1000, 1400 or 3200 mW/cm^2 irradiance levels with shortest curing times recommended resulted in unsatisfactory DC and KHN levels. LED LCU with high and extra high irradiance levels (1400 and 3200 mW/cm^2) can result in high DC and KHN levels when used adequately. Xtra Power mode (3200 mW/cm^2) used on shortest curing time (3 seconds) resulted in significantly lower mechanical properties and for that reason it is not recommended to be used.